Determination of the equivalent structural properties of a composite hydrofoil

Antoine Faye, Nicolas Carrere, Matthieu Sacher, Hauville Frédéric, Alain Nême

Determination of the equivalent structural properties of a composite hydrofoil

A.FAYE[1], N.CARRERE[2], M.SACHER[3], F.HAUVILLE[4], A.NÊME[5],

1. antoine.faye@ensta-bretagne.org
2. nicolas.carrere@ensta-bretagne.fr
3. matthieu.sacher@ensta-bretagne.fr
4. frederic.hauville@ecole-navale.fr
5. alain.neme@ensta-bretagne.fr

Abstract :

Since a few years, lifting surfaces such as hydrofoils have become increasingly popular in the naval industry. As examples, there are the kitefoils, the windfoils or the IMOCA 60. For moderate sailing speeds, the hydrodynamism and the structural response of a foil can be studied with a decoupled method, which means that a flow is modeled around a rigid foil, and then the structural properties of the foil are determined by taking into account the hydrodynamic forces estimated in the previous step. Nowadays, sailing ships can reach speeds around 35 to 40 knots. For such speeds, the decoupled method is not suited to study a foil because its deformations are not negligible anymore in the fluid simulation. Such foils require to be studied with Fluid-structure interactions (FSI) simulations, in order to take into account the influence of deformations on its hydrodynamic performances. To enhance a foil design, an optimization study can be realized, to do so, some keys parameters (geometric and structural) are identified and several FSI simulations are ran in order to identify the optimal set of parameters.The present work falls within this theme. To run a FSI simulation predicting a foil's efficiency, the first step is to define a method to evaluate the fluid flow around the foil and its structural response. The flow is modeled with the RANSE solver ISIS-CFD and the structural response of the foil is studied with the Finite Element Method (FEM), implemented in the software Abaqus. In a finite element analysis (FEA), a foil can be meshed with 3D, 2D or 1D elements. 3D and 2D elements give a more accurate description of the foil's structure compared to 1D elements. However, 3D and 2D FEA have way more parameters than a 1D FEA, which increases the dimension of the optimization problem to solve. It is why the foil is modeled as an equivalent beam, which is a linear distribution of structural properties equivalent to the 3D model. This modelization choice drastically reduces the number of optimization parameters relative to the foil's structure, which reduces the global cost of the optimization problem resolution.

In this frame of work, several methods exist to determine and exploit the equivalent properties of a composite beam. The purpose of this paper is to present and validate a method to model a 3D composite beam with 1D finite elements equivalent to the 3D model. It is shown in this paper that a foil modeled as an equivalent beam in a FEA has a similar behavior as a foil modeled with 2D and 3D elements.

Key Words : Equivalent beam, composite, bend-twist coupling, hydrofoils

Notation :

- BTC : Bend-Twist Coupling
- FEA : Finite Element Analysis
- CFD : Computational Fluid Fynamics
- FEM : Finite Element Method
- FSI : Fluid Structure Interaction
- RANSE : Reynold Average Navier-Stoke Equations
- RP : Reference Point
- DOF : Degree Of Freedom
- ANBA : ANisotropic Beam Analysis
- MPC : Multi-Point Constraint
- u_j^i : Translation DOF of node i along direction j
- u_j : Extrapolated translation DOF of a beam element along direction j
- θ_j^i : Rotational DOF of node i along direction j
- θ_j : Extrapolated rotational DOF of a beam element along direction j
- U_x, U_y,U_z : Translation DOF of the foil's tip
- R_x, R_y,R_z : Rotational DOF of the foil's tip
- N_i : Shape functions relative to translations
- M_i : Shape functions relative to rotations
- ξ : Curvilinear abscissa of an arbitrary point of a beam element
- E_l, E_t : Young modulus along longitudinal and transversal directions
- ν : Poisson coefficient
- G_{lt}, G_{lf}, G_{tf} : Shear modulus
- ρ : Density

1 Introduction

In high performances racing yacht design, hydrofoils are becoming more and more common. To study their performances, Fluid-structure interactions (FSI) simulations are realized, which require a numerical modelization of the fluid flow and of the foil's structural response. To do so, the structural response can be predicted with the finite element method (FEM) and the flow can be modeled with computational fluid dynamics (CFD). Hydrofoils are mostly designed with composite materials, which are characterized by anisotropic structural properties. This behavior has to be considered in the finite element analysis (FEA) in order to correctly model the deformation of a foil submitted to hydrodynamic forces. Depending on the fiber orientation in the composite material, coupling between deformations can appear. We can cite the bend-twist coupling (BTC) [1], which can have a massive impact on the incidence variation of a hydrofoil submitted to an hydrodynamic loading. It is why it is mandatory to model the anisotropic deformation mechanisms in a FSI simulation to perform an accurate prediction of the behavior of a foil evolving in a fluid flow. These FSI simulations can be used to optimize a foil's performances by varying its geometric (ex : chord, thickness) and structural (ex : fiber orientation, material) properties. To simplify the optimization problem, the structural model of the foil should have the minimum number of structural parameters. Classically, composite hydrofoils are studied with 3D and/or 2D finite elements. In this paper, a method is presented to model a composite foil with 1D beam elements equivalent to the 3D model. This method simplifies the optimization problem by reducing the number of structural parameters for the foil. It also reduces the computation times, which is important in the early steps of an optimization process, because a multitude of simulations have to be ran in order to find an optimal design.

The first chapter of this paper presents the foils considered for the study and the theoretical notions involved in the modelization of a foil as an equivalent beam. The second chapter discusses the numerical models used to describe the foil's structure (3D model and equivalent model). In the last chapter, we compare and discuss the results obtained with the different finite elements models. The purpose of this paper is to show that a composite hydrofoil can be modeled with 1D beam elements equivalent to the 3D model.

2 Determination method of the equivalent properties of a composite foil

The modelization of a foil as an equivalent beam is considered because it is a slender structure comparable to a beam. In most cases, its span is significantly larger than the dimensions of its section. The present study is limited to straight foil without initial twist. In the present work, FEA are performed with the commercial software Abaqus [2] developed by "Dassault Systèmes".

2.1 Foils considered for the study

To assess and illustrate the method presented in this paper, we have 4 foils with the same geometries but with different fiber orientations. These 4 foils are shown in the figure 1.

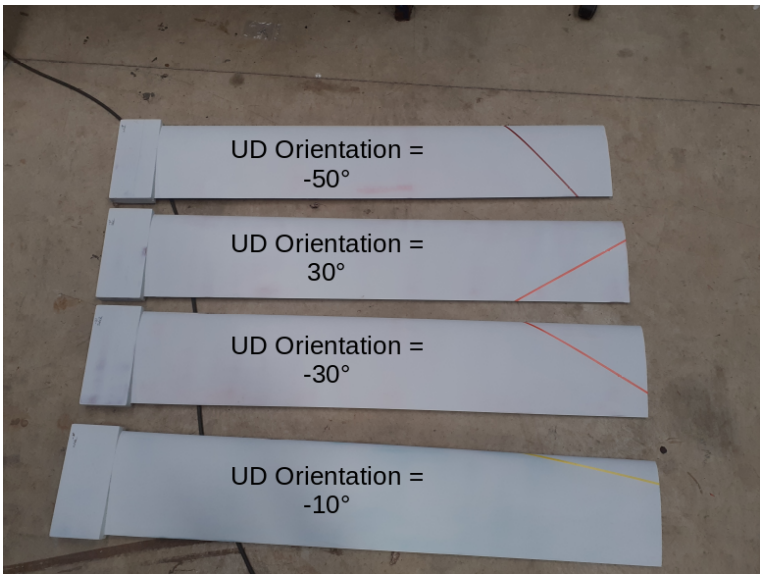

FIGURE 1: Foils considered for the study

These four foils have been constructed with the same mold and are composed of an Airex web, a ply of glass taffeta a unidirectional (UD) glass ply. Between this four foils, only the UD orientation changes, the tested orientations are ($-10°$, $-30°$, $30°$ et $-50°$). The fiber orientations are illustrated in the figure 1 with a color mark, the fiber are oriented such as the foil's extrados is symmetric to its intrados. The different orientations result in different stiffnesses (flexural, torsional ...) and different coupling (BTC, extension-torsion coupling ...) intensities. The expected structural behaviors of the foils are gathered in the the table 1. A similar work is realized in [3], the difference with the present work is the method used to determine the equivalent structural properties of a composite foil. For example, in [3], the BTC intensity of the beam is extracted from experimental data whereas in our case, it is computed with the section analysis functionality provided in Abaqus 2022.

The studied foils are straight and prismatic and their geometry is a NACA0015 (chord = 25 cm) extruded on a 1.375 m distance. Their structural properties are detailed in the table 2 and illustrated in the figure 2. The mechanical properties of the materials constituting the foils are presented in the tables 3 and 4.

UD ply orientation	Expected stiffness	Expected BTC intensity
$-10°$	high	low
$-50°$	low	medium
$-30°$	medium	high
$30°$	medium	high

TABLE 1: Expected structural behaviors of the 4 foils

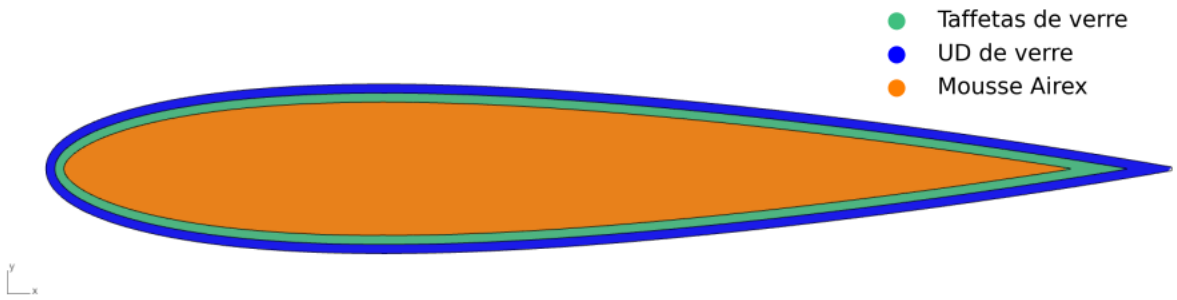

FIGURE 2: Cross section of the foils

Chord (m)	Span(m)	Taffeta ply thickness (mm)	UD ply thickness (mm)
0.250	1.375	9.45E-02	3.27E-01

TABLE 2: Geometric properties of the foils

Material	E_l (GPa)	E_t (GPa)	ν	G_{lt} (GPa)	G_{lf} (GPa)	G_{tf} (GPa)	ρ (kg/m^3)
Taffeta	16.0	16.5	0.108	1.81	1.81	0.9	1625
UD	27.4	5.1	0.348	1.81	1.81	0.9	1625

TABLE 3: Mechanical properties of the materials constituting the foils's skin

Material	E (MPa)	ν	ρ (kg/m^3)
Airex Foam	25.0	0.400	60

TABLE 4: Mechanical properties of the Airex web

2.2 Determination of the equivalent beam properties

To characterize the mechanical behavior of a foil, the 3D structural problem can be decomposed into a set of 2D problems and a 1D finite element analysis. To do so, the main steps are :

- Evaluation of the foil's sections properties (2D problems)
- Reconstruction of equivalent beam elements and FEA (1D problem)
- Reconstruction of 3D stresses and displacements from the stresses and displacements obtained with the equivalent beam model

The first step is the characterization of the foil's sections structural properties along its span. The difficulty of this step is to find equivalent properties of an anisotropic and inhomogeneous composite section.

As a starting point, we have a 3D geometry with partitions for each different regions (UD, taffeta and web in the present work). This geometry must be cut in a multitude of sections along its span, this is illustrated in the figure 3. Obviously, for a prismatic foil, a single cut is required because the section is constant along its span. The number of cuts should be adapted according to the foil's geometric and structural variations along its span.

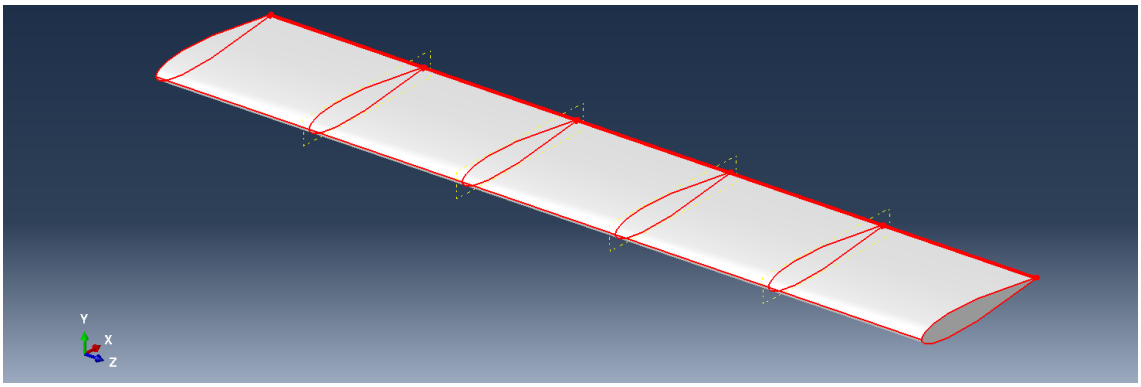

FIGURE 3: Illustration of the studied foil with six cuts

A centerline has to be defined for the equivalent beam. As a first approximation, this line goes through the geometric centers of the sections. This location is then corrected in order to have a centerline going through the shear centers of each section. The shear center of a section is the point where any load can be applied without inducing any twist. The computation of the shear center is done during the next step, which is the section analysis. For this step, the section is meshed and and its structural properties are integrated over its surface. To do so, we use Abaqus 2022 and the open source software ANBA ([4]), the theory behind the section analysis implemented in Abaqus can be find in [5]. We need to use ANBA to determine the shear center of the section, because Abaqus can not do it if there are couplings in the material. In the present work, we run a first section analysis with ANBA to compute the shear center of the section and then, we run a second section analysis with Abaqus 2022 to determine the equivalent properties of the section. The properties of the section are evaluated according to the shear center of the section. In Abaqus, we use the triangular elements WARPF2D3 allowing us to easily mesh complex sections and consider the anisotropic properties of the materials composing the foil's sections. A meshed section example is shown in the figure 4.

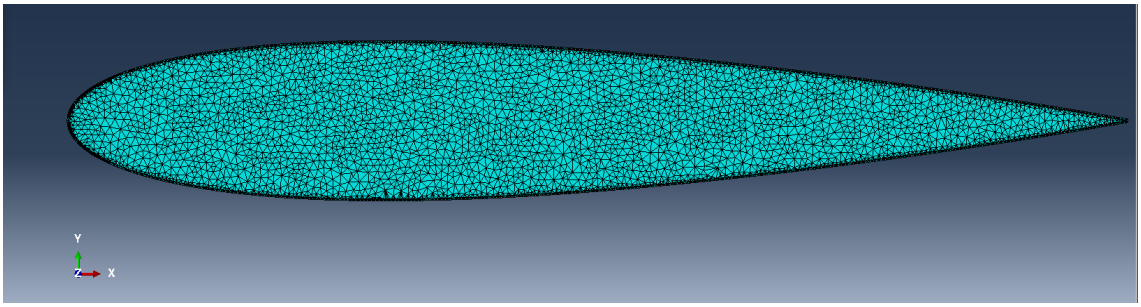

FIGURE 4: Triangular mesh of the foil's section

When the section analysis is over, we obtain, for each section, a Timoshenko stiffness matrix representative of the equivalent structural properties of the section. This matrix relates the section's forces to its strains, such as :

$$\begin{pmatrix} F_1 \\ F_2 \\ F_3 \\ M_1 \\ M_2 \\ M_3 \end{pmatrix} = \begin{pmatrix} K_{11} & K_{12} & K_{13} & K_{14} & K_{15} & K_{16} \\ K_{12} & K_{22} & K_{23} & K_{24} & K_{25} & K_{26} \\ K_{13} & K_{23} & K_{33} & K_{34} & K_{35} & K_{36} \\ K_{14} & K_{24} & K_{34} & K_{44} & K_{45} & K_{46} \\ K_{15} & K_{25} & K_{35} & K_{45} & K_{55} & K_{56} \\ K_{16} & K_{26} & K_{36} & K_{46} & K_{56} & K_{66} \end{pmatrix} \begin{pmatrix} \gamma_{11} \\ \gamma_{12} \\ \gamma_{13} \\ \kappa_1 \\ \kappa_2 \\ \kappa_3 \end{pmatrix} \tag{1}$$

In the present coordinate system (see figure 3), the subscript 1 corresponds to the z direction, the subscript 2 corresponds to the x direction and the subscript 3 corresponds to the y direction. In this matrix, we can identify some terms informing us about the mechanical properties of the equivalent beam element that is constructed from this matrix. The meanings of the diagonal terms of this matrix are detailed bellow :

- K_{11} : Axial stiffness
- K_{22}, K_{33} : Shear stiffness
- K_{44} Torsional stiffness
- K_{55}, K_{66} : Flexural stiffness

We can also identify the K_{45} and K_{46} terms to quantify the intensity of the BTC. There are other couplings in the material (ex : extension-torsion coupling, K_{14}) but we mainly focus on the BTC because it has a bigger influence than the other couplings in the present work.
The section analysis also computes the mass matrix, the transverse shear center and the warping functions of the sections. The warping functions are used to compute the deformation of a section of a deformed equivalent beam. The next step is to reconstruct a beam element from the section matrix computed during the section analysis. The reconstructed beam element must be able to model the couplings in the material. To do so, the section matrix can be integrated along the length of the beam element, as explained in [6]. In the present work, we use Abaqus 2022 to construct the equivalent beam as an assembly of beam elements. Then, boundary conditions and loads are defined and a FEA is performed. After the FEA, the equivalent beam has a deformed position, each of its nodes is associated to a translation and a rotation. The deformed 3D beam geometry can be extrapolated from these displacements and rotations. To do so, we use the shape functions of a Bernoulli beam element, which are defined as :

$$\begin{pmatrix} u_1 \\ u_2 \\ u_3 \\ \theta_1 \\ \theta_2 \\ \theta_3 \end{pmatrix} = \begin{pmatrix} N_1 & 0 & 0 & 0 & 0 & 0 & N_2 & 0 & 0 & 0 & 0 & 0 \\ 0 & N_3 & 0 & 0 & 0 & N_5 & 0 & N_4 & 0 & 0 & 0 & N_6 \\ 0 & 0 & N_3 & 0 & -N_5 & 0 & 0 & 0 & N_4 & 0 & -N_6 & 0 \\ 0 & 0 & 0 & M_1 & 0 & 0 & 0 & 0 & 0 & M_2 & 0 & 0 \\ 0 & 0 & -M_3 & 0 & M_5 & 0 & 0 & 0 & -M_4 & 0 & M_6 & 0 \\ 0 & M_3 & 0 & 0 & 0 & M_5 & 0 & M_4 & 0 & 0 & 0 & M_6 \end{pmatrix} \begin{pmatrix} u_1^1 \\ u_2^1 \\ u_3^1 \\ \theta_1^1 \\ \theta_2^1 \\ \theta_3^1 \\ u_1^2 \\ u_2^2 \\ u_3^2 \\ \theta_1^2 \\ \theta_2^2 \\ \theta_3^2 \end{pmatrix} \tag{2}$$

This matrix relates the displacement of an arbitrary point of a beam element with the displacements of its two nodes. This point's position is described by a local adimensional variable ξ varying between 0 and 1. The different shape functions depends on this variable and are given bellow :

$$N_1(\xi) = 1 - \xi \qquad N_2(\xi) = \xi \tag{3}$$

$$N_3(\xi) = 1 - 3\xi^2 + 2\xi^3 \qquad N_4(\xi) = 3\xi^2 - 2\xi^3 \tag{4}$$

$$N_5(\xi) = L(\xi - 2\xi^2 + \xi^3) \qquad N_6(\xi) = L(-\xi^2 + \xi^3) \tag{5}$$

$$M_1(\xi) = 1 - \xi \qquad M_2(\xi) = \xi \qquad M_3(\xi) = -\frac{6}{L}(\xi - \xi^2) \tag{6}$$

$$M_4(\xi) = \frac{6}{L}(\xi - \xi^2) \qquad M_5(\xi) = 1 - 4\xi + 3\xi^2 \qquad M_6(\xi) = -2\xi + 3\xi^2 \tag{7}$$

In the equations above, L is the length of the beam element. This approach is only valid if the warping of the sections is negligible. Otherwise, the 3D deformation must be computed with the warping functions computed during the section analysis. To study a foil, the stresses in the section should also be computed with the warping functions to evaluate the maximum stresses in the structure. The stresses computed on the equivalent beam elements are not sufficient to check the structural integrity of the foil because it does not take into account the warping of sections and the maximum stress does not necessarily occur at the shear center of the sections. The determination of the maximum stress with the equivalent beam method is not discussed in this paper.

3 Numerical models

In this section, we present the two numerical models predicting the deformation of the foils under a given load case.

3.1 Abaqus 3D

3.1.1 Mesh

In the reference 3D Abaqus FEA, the foil is decomposed in two parts, a first one containing the Airex web, meshed with 3D elements. The second part is meshed with 2D elements and represents the foil's skin (taffeta and UD). The 2D elements used for the skin drastically reduce the size of the structural mesh because the skin is not discretized along its thickness. The 3D elements used to model the web are 8 node brick elements C3D8R. The optimal number of elements necessary to describe correctly the web's behavior is 675 000. The meshed web is illustrated in the figure 5. The 2D elements used for the skin are triangular shell elements STRI3. On these elements, a "composite layup" is defined to specify the thickness of the layers and the fiber orientation. The optimal mesh for the skin is constituted of 60 000 elements (6).

3.1.2 Constraints, boundary conditions and loading case

In Abaqus, a "Tie" constraint is defined to link the skin to the web. This constraint imposes the motion of the web's surface to be the same as the foil's 2D skin.The 4 foils studied in this paper will be experimentally studied to assess the numerical models. In these experiments, the "heel" of the foil

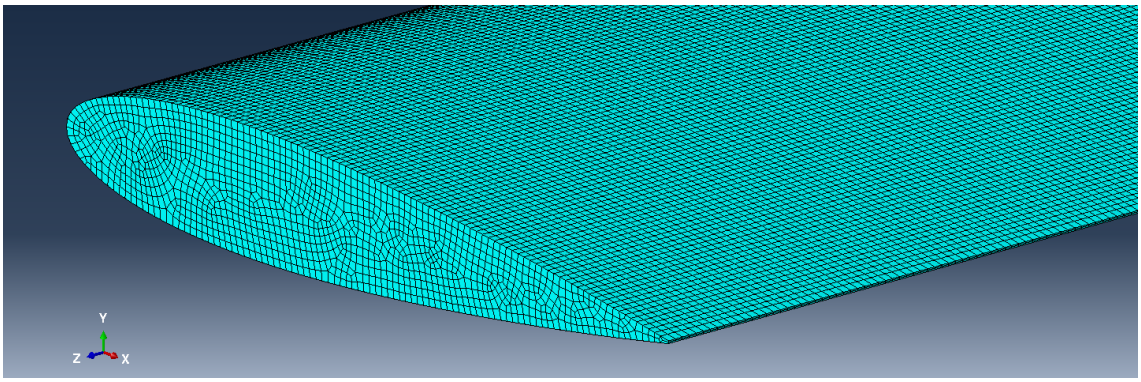

FIGURE 5: Structural mesh of the foil's web

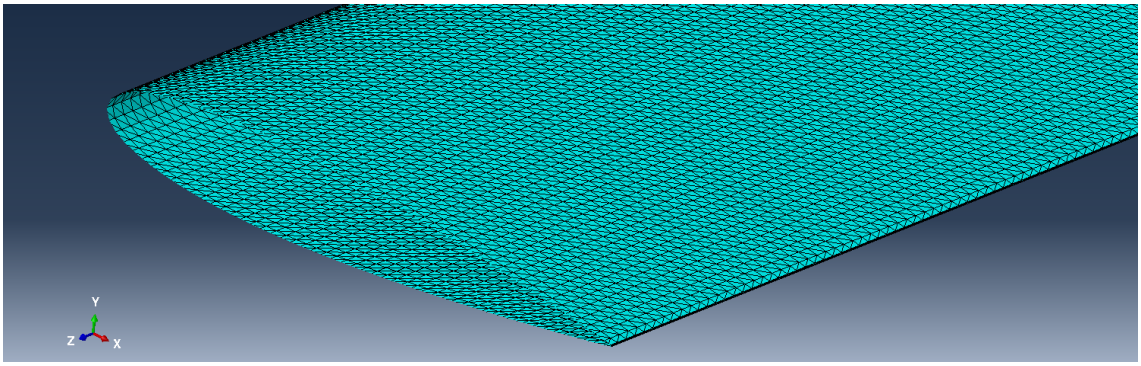

FIGURE 6: Structural mesh of the foil's skin

(see figure 1) will be clamped and concentrated loads will be applied at several locations along its span and chord. To apply the loading, a "clamping ring" will be used. It will be movable along the foil's span and a mass will be fixable at several locations along the chord. To illustrate this, we show in the figure 7 a similar experimental device used in [1]. To foresee the experimental campaign, the loading case

FIGURE 7: Experimental device used to study the mechanical properties of a foil [1]

modeled in Abaqus have to be as representative as possible of the loading in the experimental setup. To do so, the foil's skin is partitioned in order to represent the contact surface between the "clamping ring" and the skin. Then, with a multi-point constraint (MPC), this surface is constrained to follow a reference point where a concentrated load will be applied. To model the clamping of the foil's "heel", the displacement of the skin and the web are constrained to be null in z=0. This is illustrated in the figure 8 with the blue and orange arrows. In this figure, the loading case is also represented, the partition of the skin is defined between the two yellow plane and the reference point (RP) is located at 1.3 m from the clamping and 20 cm from the leading edge.

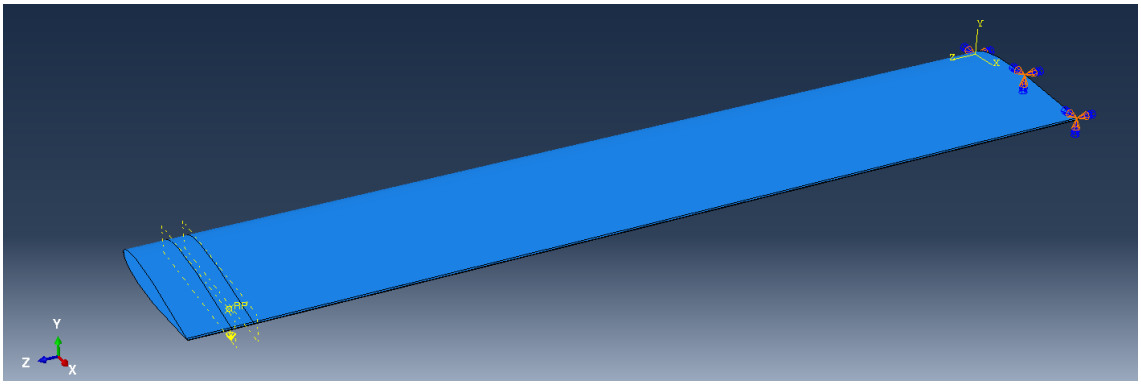

FIGURE 8: Illustration of the loading case and boundary conditions in Abaqus for the 3D model

3.2 Abaqus 1D

Because the foils are prismatic, a single section analysis is performed per foil. In this section, we detail the modelization of the foil as an equivalent beam with Abaqus 2022.

3.2.1 Section Analysis

The integration of the section's mechanical properties is made with the mesh shown in 4. The elements used to mesh the section are triangular elements WARPF2D3, which are able to model the out of plane warping of the section. This component of the warping have to be considered to study composite materials. For the anisotropic materials of the section, an orientation must be defined in Abaqus to model the fiber orientation. During the section analysis, the section's origin must be the shear center of the section because the centerline of the equivalent beam go through this point. The location of the shear center is determined during a preliminary section analysis realized with the software ANBA.

3.2.2 Reconstruction of the equivalent beam

The equivalent foil modeled in Abaqus is made of 90 Timoshenko beam elements B31 (2 nodes linear element). The nodes of the beam elements go through the shear centers of the sections of the foil. A clamping condition is defined at the base of the foil (z=0) and a concentrated load is applied as in the 3D model. To do so, a reference point (RP) is defined to model the point of application of the concentrated load.Then, with a MPC, the RP is rigidly linked to the beam elements located between z=1.285 m and z = 1.315 m. Which corresponds to the location of the clamping ring along the foil's span. The loading case and the boundary condition are shown in figure 9.

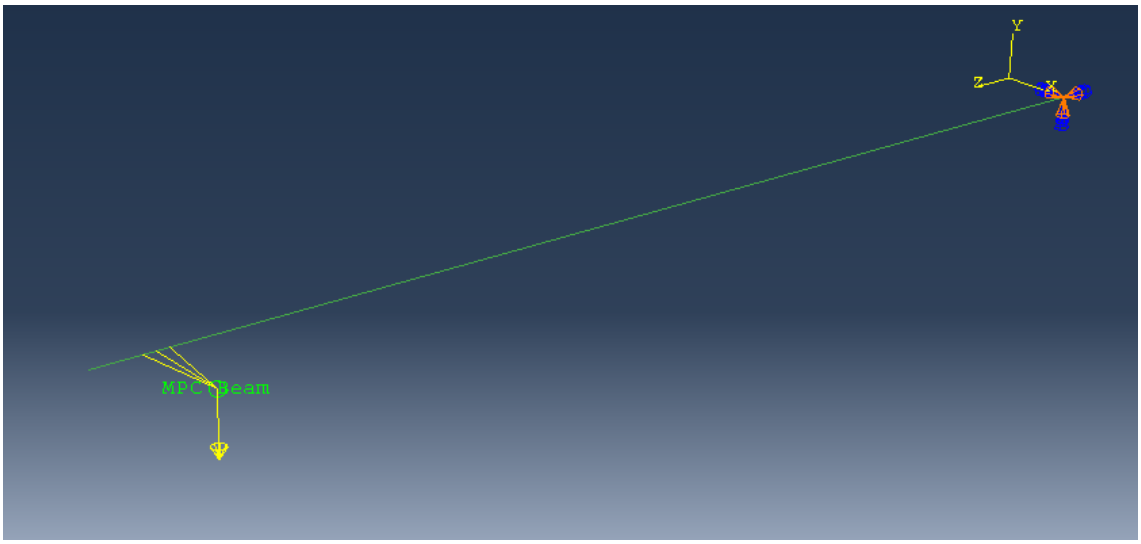

FIGURE 9: Illustration of the loading case and boundary conditions in Abaqus for the equivalent beam

4 Results

In this section, we show and discuss the results obtained with the 4 foils with the two numerical models. We remind that the orientation of the UD fibers are the only variable in our study, it takes the values ($-10°$, $-30°$, $30°$ et $-50°$). To compare the models, we consider the loading case illustrated in the figures 8 and 9 with a dead load of -147.15 N oriented along the y axis applied at (0.2, 0 ,1.3) m. In the Earth's gravitational field, it corresponds to a mass of 15 kg suspended to the foil.

4.1 Computation of the shear centers

Here, we present the shear centers computed with the solver ANBA. The positions are expressed according to the the leading edge with the coordinate system of the figure 2. The results are gathered in the table 5. We remind that the shear centers are used to define the centerline of the equivalent beam.

UD orientation	Shear center (mm)
$-10°$	(94.46 , 0.0)
$-50°$	(92.56 , 0.0)
$-30°$	(92.11 , 0.0)
$30°$	(92.11 , 0.0)

TABLE 5: Shear centers of the 4 foil sections

4.2 Comparison of the 3D and equivalent model

For each foil, FEA are performed with the two different models presented earlier. For each case, the foils's tip displacements are compared. For the 3D model, the tip displacement is computed as the mean displacement of the skin's nodes at the foil's tip. From this set of points, the section's rotation is also computed. To do so, we record the initial and deformed positions of 4 points of the foil's tip section. The 4 points are the leading edge, the trailing edge, the highest point of the extrados and the lowest point of the intrados. From these points, a frame can be determined for the initial and deformed sections, from which we deduce a rotation matrix. From this matrix, we can compute the rotation parameters R_x, R_y

and R_z used to describe the rotation of the nodes of a beam element in Abaqus. The tip displacements for each fiber orientation are given in the tables 6, 7, 8 and 9.

	U_x (m)	U_y (m)	U_z(m)	$R_x(^\circ)$	$R_y(^\circ)$	$R_z(^\circ)$
Abaqus 3D	-4.871E-02	-3.312E-01	6.148E-03	2.031E+01	1.327E-01	1.632E+00
Abaqus 1D	-5.085E-02	-3.398E-01	5.003E-03	2.068E+01	5.385E-02	1.628E+00
Difference	4.4%	2.6%	18.6%	1.8%	59.4%	0.3%

TABLE 6: Tip displacement of the foil for the orientation -50°

	U_x (m)	U_y (m)	U_z(m)	$R_x(^\circ)$	$R_y(^\circ)$	$R_z(^\circ)$
Abaqus 3D	-2.501E-02	-2.375E-01	9.883E-03	1.450E+01	4.822E-02	5.260E+00
Abaqus 1D	-2.728E-02	-2.504E-01	1.080E-02	1.492E+01	2.280E-02	5.645E+00
Difference	9.1%	5.4%	9.3%	2.9%	52.7%	7.3%

TABLE 7: Tip displacement of the foil for the orientation -30°

	U_x (m)	U_y (m)	U_z(m)	$R_x(^\circ)$	$R_y(^\circ)$	$R_z(^\circ)$
Abaqus 3D	-7.324E-03	-1.299E-01	1.940E-03	7.674E+00	5.372E-02	1.192E+00
Abaqus 1D	-7.564E-03	-1.328E-01	2.473E-03	7.747E+00	6.490E-02	1.477E+00
Difference	3.3%	2.2%	27.5%	1.0%	20.8%	23.9%

TABLE 8: Tip displacement of the foil for the orientation -10°

	U_x (m)	U_y (m)	U_z(m)	$R_x(^\circ)$	$R_y(^\circ)$	$R_z(^\circ)$
Abaqus 3D	-3.285E-02	-2.732E-01	-1.550E-02	1.678E+01	2.093E-01	-9.661E+00
Abaqus 1D	-3.490E-02	-2.809E-01	-1.863E-02	1.739E+01	9.873E-02	-1.007E+01
Difference	6.3%	2.8%	20.2%	3.6%	52.8%	4.3%

TABLE 9: Tip displacement of the foil for the orientation 30°

There is a good agreement between the results obtained with the equivalent beam model and the 3D model. With the two models, the foils's mechanical behaviors are consistent with their fiber orientation. For example, the largest deflection is obtained for an orientation of -50° and the smallest is obtained for the orientation of -10°. However, some differences are important between the models, particularly for the values of U_z and R_y. In the present study, the U_z and R_y induced by the load case are small, which explains the important differences. All the displacements with a significant magnitude computed with the two methods are close.

To study a foil in a FSI simulation, it is mandatory to correctly model the incidence of the foil regarding the flow because it has a major impact on the hydrodynamic forces acting on the foil. To compare the models, we plotted the evolution of the foils's twist R_z (analog to the incidence) along their span (figure 11). In each case, the incidence of the foils along their span follows the same trend with the two models. Theses results are encouraging, it shows that the BTC is correctly modeled when using the equivalent beam approach. As a first conclusion, it seems that the foil could be modeled as an equivalent beam in a FSI simulation. To confirm this, computations should be ran considering a hydrodynamic loading.

To further illustrate the results, figure 10 shows the deformed foils obtained with the 2 models. The deformed geometries are similar but we can notice that the differences between the models increase with

the amplitude of the deformation. In the 3D model, when deformations are important enough, some locals phenomenons changing the local orientations of the material may appear, which directly impacts the stiffness and coupling of the materials. This kind of phenomenon can't be modeled in the equivalent beam because the section analysis is only performed once before the FEA.

The different foil behaviors can be related to their section stiffness matrix K (1). The terms of the section matrices of the 4 foils are gathered in the table 10. In this table, the axial and flexural stiffnesses K_{11}, K_{55} and K_{66} are decreasing when the fibers orientation are getting away from 0°, which is an expected behavior when studying composite materials. This explains why the foil with the $-50°$ orientation has the largest deflection and the foil with the $-10°$ orientation has the smallest one.

Another interesting result is the values of the BTC term K_{45}, for the foils with negative fiber orientation, it is positive whereas it is negative for the $30°$ orientation. This means that the torsion induced by the flexion for the $30°$ orientation has an opposite sign to the torsion induced for positive UD orientations. This affirmation can be checked in the figure 11 where the incidence variations of the foils are positive for the negative UD orientations and negative for the $30°$ orientation.

To illustrate the time saved when using the equivalent beam modelization, the table 11 gathers the different computational times for the FEA performed on the foil with the $-50°$ orientation. This foil is considered because it has the largest deflection and therefore the slowest convergence rate of all the computations. The reference 3D FEA is realized with 10 processors and despite that, the equivalent beam method is still 250 times faster. This result illustrates the benefits of the equivalent beam method to save time in structural computations. Which is important when solving an optimization problem where lots of computations have to be ran. The time saved by the equivalent beam method is even greater in FSI computations because the section analysis is only performed once at the beginning of the computation, and the table 11 shows that most of the computational time of the equivalent beam method is spent on the section analysis. Obviously, the section analysis step would be longer if the foils were not prismatic.

UD orientation	$-50°$	$-30°$	$-10°$	$30°$
K_{11} (N)	1.912E+06	3.159E+06	5.140E+06	3.159E+06
K_{22} (N)	8.051E+05	8.264E+05	4.529E+05	8.264E+05
K_{33} (N)	7.652E+04	6.826E+04	6.557E+04	6.826E+04
K_{44} $(N.m^2)$	6.182E+02	6.829E+02	3.546E+02	6.829E+02
K_{55} $(N.m^2)$	3.355E+02	5.903E+02	9.514E+02	5.903E+02
K_{66} $(N.m^2)$	1.126E+04	1.560E+04	2.835E+04	1.560E+04
K_{45} $(N.m^2)$	1.031E+02	3.365E+02	2.143E+02	-3.365E+02

TABLE 10: Comparison of the section stiffness matrices computed for the 4 foils

	Processors number	Computational time (s)
Abaqus 3D	10	1.8E+04
Section Analysis	1	7.1E+01
Abaqus 1D	1	1.4E-01

TABLE 11: Computational cost of the FEA with the two methods for the $-50°$ orientation

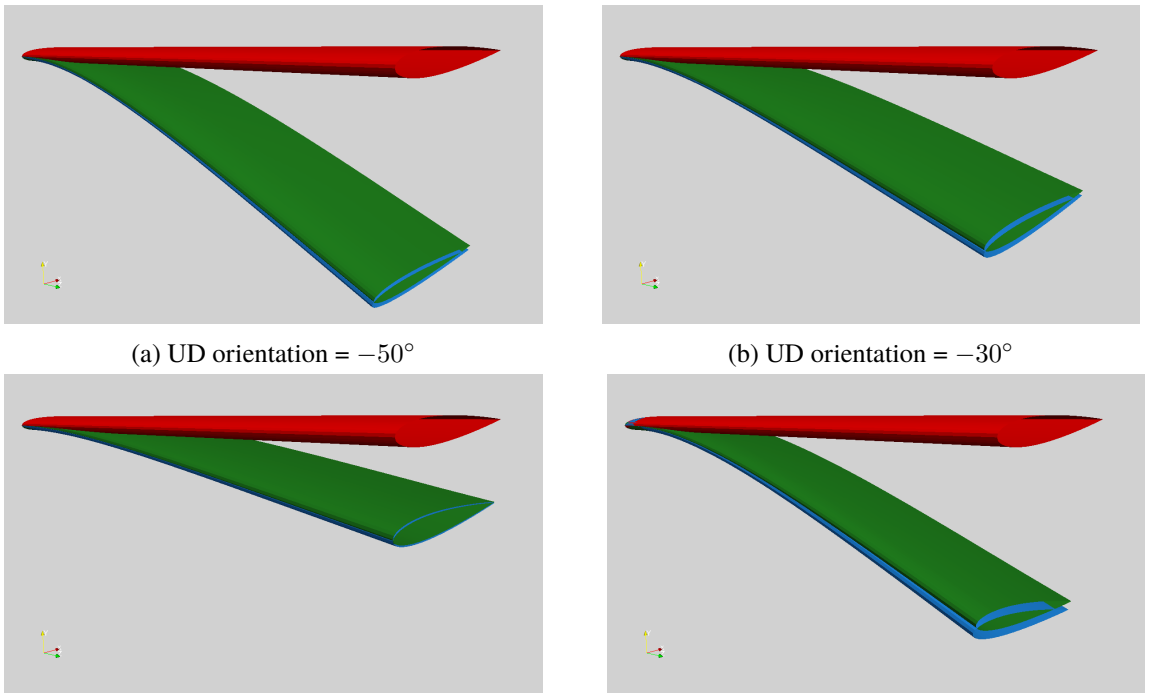

(a) UD orientation = $-50°$ (b) UD orientation = $-30°$

(c) UD orientation = $-10°$ (d) UD orientation = $30°$

FIGURE 10: Comparison of the deformed foils computed with the two models ((●) : Underformed beam, (●) : Equivalent beam, (●) : Abaqus 3D)

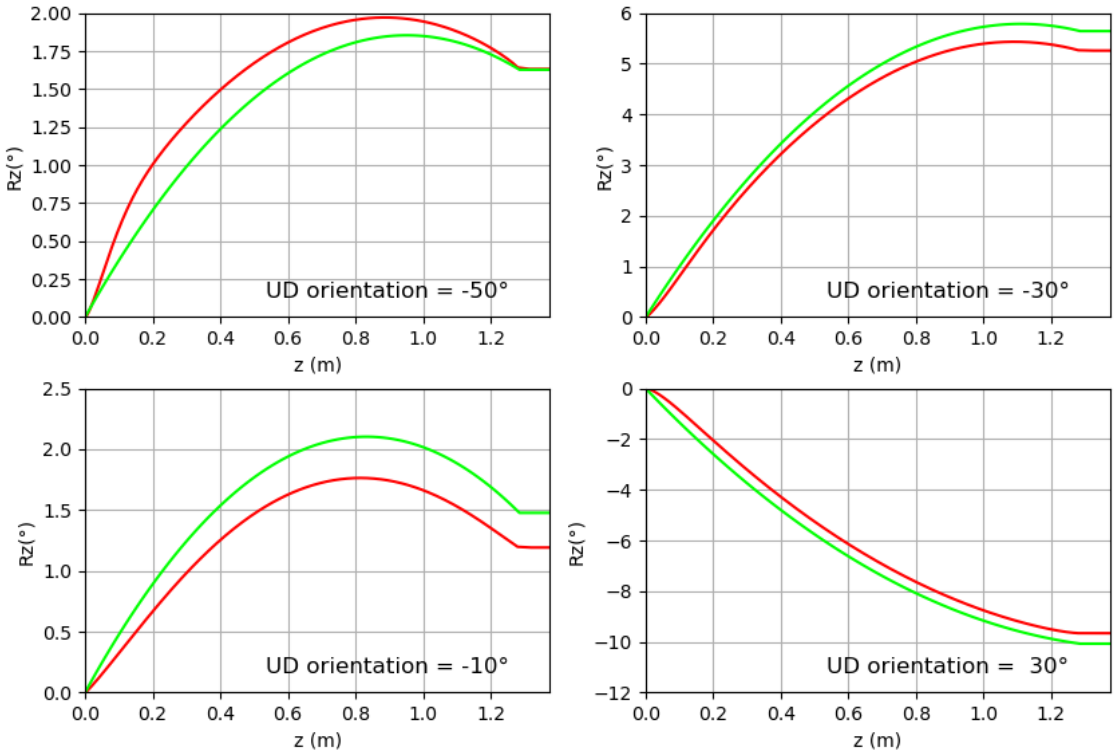

FIGURE 11: Incidence variation along the span of the foils computed with the two models ((●) : Equivalent beam, (●) : Abaqus 3D)

5 Conclusion

This paper presented a method to model a composite hydrofoil as an equivalent beam. This works is performed to determine if an hydrofoil could be optimized with FSI simulations considering the equivalent beam approach. This approach reduces the dimension of the optimization problem and the computational cost of its resolution. The method is decomposed in two main parts, firstly, the sections of the foil are analyzed all along its span with the section analysis tools provided by Abaqus 2022 and ANBA. And then, from the results obtained with the section analysis, an equivalent beam is defined as an assembly of 1D finite beam elements and a FEA can be achieved. Then, the 3D geometry of the deformed foil can be determined from the equivalent beam displacements. The equivalent beam method is able to model couplings in the materials, such as bend-twist coupling or extension-twist coupling. The results obtained with an equivalent beam are close to the one obtained with a classical finite element representation of the foil (3D+2D elements). The deformations (rotations + translations) are correctly modeled even if some differences between the two models appear for important deformations. The results are encouraging and let us think that the equivalent beam model is adapted to realize FSI simulations on an hydrofoil to evaluate its performances. As a future work, computations should be performed considering a hydrodynamic loading applied on the foil. Also, this method should be validated with more complex foils, with varying geometric and structural properties for example. It would also be relevant to explore the validity of the equivalent beam model for initially twisted and curved hydrofoils. Finally, the maximum stresses computed with the two models should be investigated, to check if a hydrofoil's structural integrity could be assessed with the equivalent beam method.

References

[1] V. Temtching Temou. *Étude expérimentale et numérique des interactions fluides-structures sur des hydrofoils flexibles en composite*. PhD thesis, UBO, 2020.

[2] Abaqus documentation. `https://abaqus-docs.mit.edu/2017/English/SIMACAEEXCRefMap/simaexc-c-docproc.htm`, 2017.

[3] V. Temtching Temou, B. Augier, and B. Paillard. Hydro-elastic response of composite hydrofoil with fsi. *Ocen engineering*, 2021.

[4] R. Feil, T. Pflumm, and M. Bortolotti, P. Morandini. A cross-sectional aeroelastic analysis and structural optimization tool for slender composite structures. *Composite structures*, 2020.

[5] S. Han and O. Bachau. Nonlinear three-dimensional beam theory for flexible multibody dynamics. *Multibody System Dynamics*, 2014.

[6] A.R. Stäblein and M.H. Hansen. Timoshenko beam element with anisotropic cross-sectional properties. In *ECCOMAS Congress*, June 2016.